Scripta Materialia 152 (2018) 132–136

Contents lists available at ScienceDirect

Scripta Materialia

journal homepage: www.elsevier.com/locate/scriptamat

Regular article

Fabricating ultrafine grain by advanced thermomechanical processing on low-carbon microalloyed steel

Ba Li [a,*], Qingyou Liu [a], Shujun Jia [a], Yi Ren [b], Bing Wang [a]

[a] Central Iron & Steel Research Institute, Beijing 100081, China
[b] Iron & Steel Research Institutes of Ansteel Group Corporation, Anshan, Liaoning 114009, China

ARTICLE INFO

Article history:
Received 23 February 2018
Received in revised form 8 April 2018
Accepted 20 April 2018
Available online xxxx

Keywords:
Intercritical deformation
Deformation induced ferrite transformation
Continuous dynamic recrystallization
Ultrafine grain
Subgrains

ABSTRACT

The ultrafine grain with the effective grain size of 1.10 μm was fabricated by intercritical deformation on low-carbon microalloyed steel, which was finer than the deformation induced ferrite transformation (DIFT) at 1.55 μm. During intercritical deformation, the DIFT process was enhanced, showing a colony distribution of the refined grains. Meanwhile, the continuous dynamic recrystallization of pro-eutectoid ferrite was developed by both the subgrains progressively trapping dislocations and the serrated boundary pinching off the elongated grains. These processes were directly observed through the grain average misorientation maps of electron back-scattered diffraction and confirmed by transmission electron microscopy micrographs.

The advanced thermomechanical processing (ATP) technology is an effective way to acquire the excellent comprehensive property with low cost by achieving the microstructure refinement on the low-carbon microalloyed steel. For an intrinsic view, the grain refinement mechanism of the ATP is realized by combining the following phenomenon [1,2]: (i) dynamic recrystallization (DRX) of austenite i.e. deformation in the recrystallization region of austenite; (ii) extended phase transformation of the deformed-austenite with the abundant deformation bands i.e. deformation in the non-recrystallization region of austenite; (iii) deformation induced ferrite transformation (DIFT) by deformation in the low-temperature interval of the austenite non-recrystallization region; and (iv) DRX or dynamic recovery (DRV) of ferrite i.e. warm or cold deformation in the ferrite region. During these processes, the DIFT technology i.e. heavy deformation between A_{e3} and A_{r3} obtains an extremely efficient grain refinement, demonstrating its potential for the industrial application [3–8]. Therefore, more attention is attracted to the study on their thermomechanical procedures [5,8]. However, the intercritical deformation (ID) technology, deformation at ferrite + austenite (α + γ) phase regions, can produce finer grains than the DIFT technology through both the γ-DIFT and α-DRX [9,10]. For example, Zhao et al. produced ultrafine grains with 0.46 μm on the 10Ni-0.1C steel by ID at 520 °C resulting from DRX that occurs on the dynamically transformed ferrite [11]. However, many investigators reported that only the continuous DRX (cDRX) of the pro-eutectoid ferrite take place during ID [12–15], while other researchers found that the DIFT also occurs [16,17]. Additionally, Zhang et al. pointed out that the DIFT and cDRX dominates the high and low temperature interval of the intercritical region in low-carbon Cu-P-Cr-Ni-Mo weathering steel, respectively [18]. For the work conducted by Anish Karmakar et al., the high and low temperature interval is dominated by the cDRX and DRV of ferrite in low-carbon microalloyed steel, respectively [19]. Therefore, the formation mechanism of the ultrafine grain in this region is extremely intricate and remains unclear. Moreover, the grain refinement comparison between the DIFT and ID has not received much attention. In this paper, two-stage hot compression tests were performed on the microalloyed steel to comparatively study the DIFT and ID.

The experimental steel used in this work was commercial low-carbon microalloyed steel (0.04 C, 0.28 Si, 1.54 Mn, 0.011 P, 0.002 S, 0.062 Nb, 0.014 Ti, 0.14 Mo, 0.29 Ni, Cr: 0.25, Fe: bal., (wt%)). The simulated ATP was conducted in a Gleeble 1500 simulator. The samples were 20 mm long cylindrical tubes with a diameter of 8 mm. The deformation tests schedule is displayed in Fig. 1. The samples were initially austenitised at 1180 °C for 300 s, followed by cooling to 980 °C. The first-stage uniaxial compressive strain of 0.36 (30% reduction) was then performed. The rate of heating, cooling and strain rate was 10 °C/s, 5 °C/s and 1 s^{-1}, respectively. Here, the rise of A_{r3} resulting from the first-stage deformation was taken into account. The A_{r3} (720 °C) was determined by dilatometric study using the same procedure as the first-stage deformation. The A_{e3} (840 °C) was calculated with Thermo-Calc software. The samples were then respectively cooled to 820 °C and 690 °C. The second-stage compressive strain of 0.69 (50% reduction) was conducted. After deformation, the samples were cooled with

* Corresponding author.
E-mail address: balicugb@sina.com. (B. Li).

https://doi.org/10.1016/j.scriptamat.2018.04.028
1359-6462/

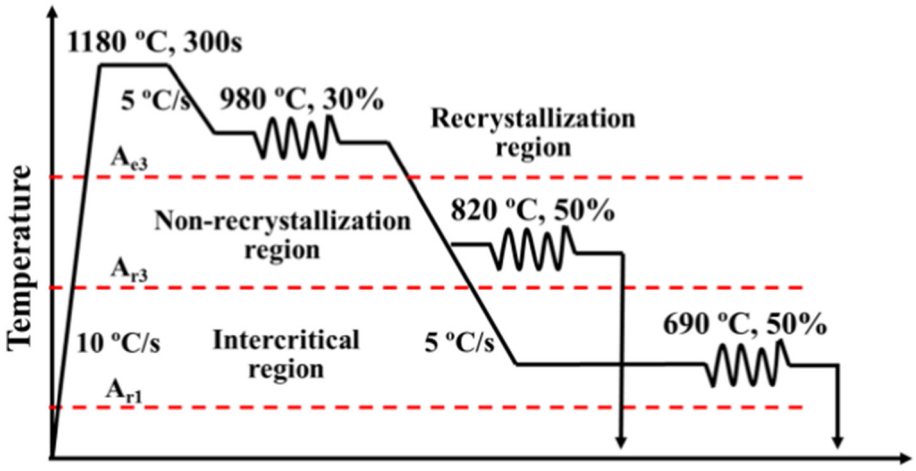

Fig. 1. Schematic diagram of ATP conditions.

water injection immediately. The microstructure before the second-stage deformation was also prepared via water cooling for comparisons. The microstructure at the center, on a cross section of the compressed samples, was observed via scanning electron microscopy (SEM, S-4300), transmission electron microscopy (TEM, H-800) and electron back-scattered diffraction (EBSD, Nordlys F+). The SEM samples were ground, polished, and then etched with a 4% Nital solution. Thin foil samples with a diameter of 3 mm for both TEM (30–50 μm thickness) and EBSD (80–100 μm thickness) were electropolished by a twin-jet electropolisher, in an electrolyte that consisted of 6% perchloric acid and 94% methanol, below −30 °C. Notably, the EBSD sample was not sprayed penetration.

As shown in Fig. 2((a) and (b)), the microstructure of the samples before deformation at 820 °C and 690 °C were entire martensite and pro-eutectoid ferrite + martensite, respectively. The martensite was phase-transformed from the undercooling austenite. After 0.69 strains, the microstructures at both 820 °C and 690 °C were remarkably refined and numerous equiaxed grains replaced the expected pancake structure, as seen in Fig. 2((c) and (d)). The results indicated that microstructure restoration occurred. The stress-strain curves are provided by the inset in Fig. 2(e), which showed significant softening after reaching a peak stress during the second-stage deformation. This dynamic softening behavior and the refinement of ferrite grains were attributed to the DIFT for deformation at 820 °C. However, both the DIFT and DRV/cDRX of ferrite could be responsible for the microstructure restoration at 690 °C deformation.

The double-differentiation method was adopted to calculate the critical stress determined by the stationary point on the double-differentiation curve with respect to stress [7]. This method primarily requires the smoothing flow curve to be fitted with at least order eight polynomials. If there are two possible minima, the use of polynomials of as high as order twelve are required [20]. Therefore, the 8 to 16 order polynomials were performed, and then two minima were distinguished when the order exceeded 12, as shown in Fig. 2(e). The first and second minima were considered as the initiation of the DIFT and pro-eutectoid ferrite DRV/cDRX, respectively.

As seen in Fig. 3(a), the effective grain size, the grain enclosed by high angle grain boundaries (HAGBs), of the samples before deformation at 820 °C and 690 °C were 6.4 μm and 4.3 μm, respectively. At 690 °C, the undercooling austenite partly transformed into the pro-eutectoid ferrite, which increased the interface content that refined the entire microstructure. The effective grain size of the samples after 0.69 strains at 820 °C and 690 °C decreased to 1.55 μm and 1.10 μm, respectively. It is known that the generation of fine grains will be limited by the needs of dissipating enthalpy during fast transformation by large undercooling (such as water cooling) [21]. Therefore, the grain size of samples will not be further refined by water cooling after the second-stage deformation i.e. the grain refinement was mainly achieved during

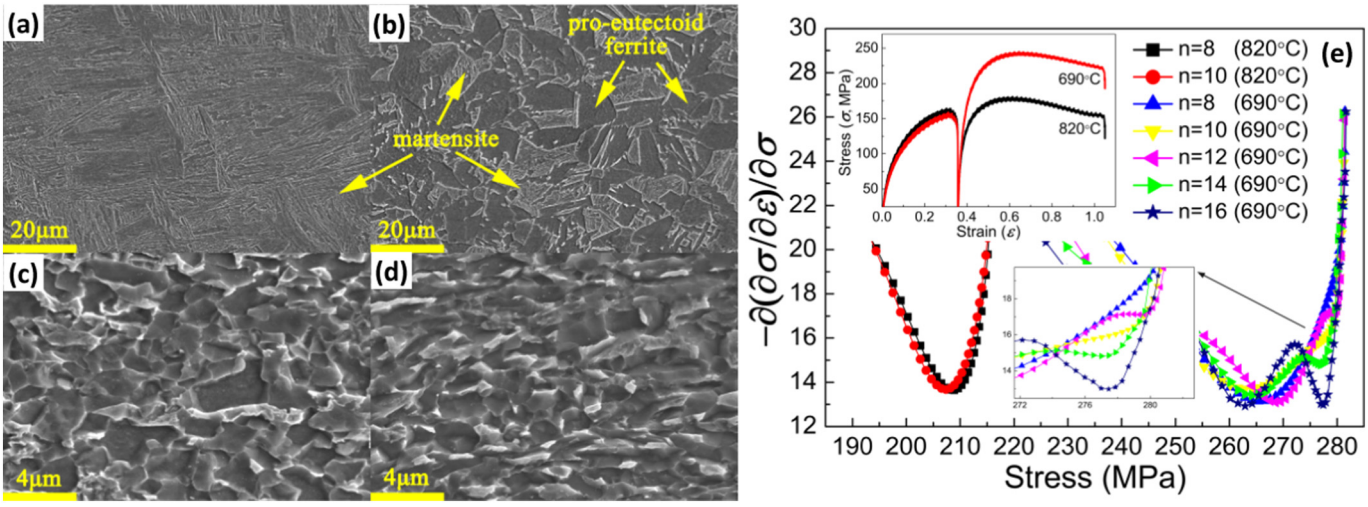

Fig. 2. SEM micrographs of 820 °C and 690 °C samples: (a, b) before deformation and (c, d) after deformation. (e) Effect of polynomial order on stress second derivative of the second-stage deformation.